

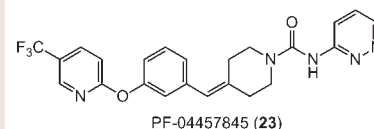
# Discovery of PF-04457845: A Highly Potent, Orally Bioavailable, and Selective Urea FAAH Inhibitor

Douglas S. Johnson,<sup>\*,†,§</sup> Cory Stiff,<sup>†,§</sup> Scott E. Lazerwith,<sup>§</sup> Suzanne R. Kesten,<sup>§</sup> Lorraine K. Fay,<sup>§</sup> Mark Morris,<sup>§</sup> David Beidler,<sup>†,§</sup> Marya B. Liimatta,<sup>§</sup> Sarah E. Smith,<sup>§</sup> David T. Dudley,<sup>§</sup> Nalini Sadagopan,<sup>§</sup> Shobha N. Bhattachar,<sup>§</sup> Stephen J. Kesten,<sup>§</sup> Tyzoon K. Nomanbhoy,<sup>||</sup> Benjamin F. Cravatt,<sup>⊥</sup> and Kay Ahn<sup>†,§</sup>

Pfizer Worldwide Research and Development, <sup>†</sup>Groton, Connecticut 06340, United States, <sup>‡</sup>Cambridge, Massachusetts 63017, United States, <sup>§</sup>Ann Arbor, Michigan 48105, United States, <sup>||</sup>ActivX Biosciences, 11025 North Torrey Pines Road, La Jolla, California 92037, United States, and <sup>⊥</sup>The Skaggs Institute for Chemical Biology and Department of Chemical Physiology, The Scripps Research Institute, 10550 North Torrey Pines Road, La Jolla, California 92037, United States

**ABSTRACT** Fatty acid amide hydrolase (FAAH) is an integral membrane serine hydrolase that degrades the fatty acid amide family of signaling lipids, including the endocannabinoid anandamide. Genetic or pharmacological inactivation of FAAH leads to analgesic and anti-inflammatory phenotypes in rodents without showing the undesirable side effects observed with direct cannabinoid receptor agonists, indicating that FAAH may represent an attractive therapeutic target for the treatment of inflammatory pain and other nervous system disorders. Herein, we report the discovery and characterization of a highly efficacious and selective FAAH inhibitor PF-04457845 (**23**). Compound **23** inhibits FAAH by a covalent, irreversible mechanism involving carbamylation of the active-site serine nucleophile of FAAH with high in vitro potency ( $k_{\text{inact}}/K_i$  and  $IC_{50}$  values of  $40300 \text{ M}^{-1} \text{ s}^{-1}$  and 7.2 nM, respectively, for human FAAH). Compound **23** has exquisite selectivity for FAAH relative to other members of the serine hydrolase superfamily as demonstrated by competitive activity-based protein profiling. Oral administration of **23** at 0.1 mg/kg results in efficacy comparable to that of naproxen at 10 mg/kg in a rat model of inflammatory pain. Compound **23** is being evaluated in human clinical trials.

**KEYWORDS** FAAH, endocannabinoid, irreversible inhibitor, clinical candidate



Fatty acid amide hydrolase (FAAH) is an integral membrane enzyme that degrades the fatty acid amide family of signaling lipids, including the endocannabinoid anandamide.<sup>1–3</sup> FAAH is a serine hydrolase that employs an unusual serine–serine–lysine catalytic triad to efficiently hydrolyze both amides and esters.<sup>4</sup> Genetic or pharmacological inactivation of FAAH leads to elevated endogenous levels of fatty acid amides<sup>5</sup> and a range of analgesic effects in various animal models of inflammation and chronic pain.<sup>6–9</sup> Importantly, these behavioral phenotypes occur in the absence of the undesirable side effects observed with direct cannabinoid receptor agonists, indicating that FAAH may represent an attractive therapeutic target for the treatment of inflammatory pain and related conditions.

Several classes of reversible and irreversible covalent FAAH inhibitors have been reported (Figure 1).<sup>8,10</sup> Electrophilic ketone inhibitors such as OL-135 (**1**) reversibly form an enzyme-stabilized hemiketal between the active-site Ser241 and the electrophilic carbonyl.<sup>11–12</sup> Carbamates such as URB597 (**2**) irreversibly inhibit FAAH by carbamylation of Ser241 with the alcohol group serving as the leaving group.<sup>13–15</sup> We and

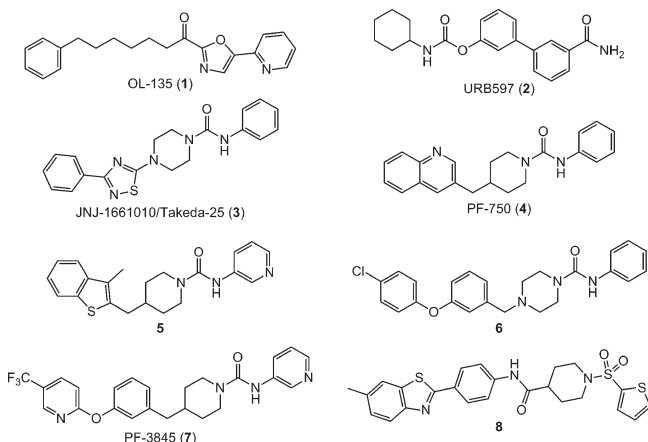
others have previously reported a series of piperidine/piperazine urea FAAH inhibitors (e.g., **3–7**).<sup>16–21</sup> Mechanistic studies revealed that PF-750 (**4**) inhibited FAAH in a time-dependent manner by covalently modifying the enzyme's active site nucleophile, despite the inherent stability of the urea functional group.<sup>16</sup> PF-750 was confirmed to be covalently attached to the Ser241 of FAAH through a carbamate linkage by a X-ray crystal structure of humanized rat (h/r) FAAH in complex with PF-750.<sup>22</sup> Additional medicinal chemistry efforts led to the identification of a more potent series of FAAH inhibitors based on a biaryl ether piperazine/piperidine urea scaffold (e.g., **6** and **7**).<sup>17,21</sup> The prototype from this series, PF-3845 (**7**), inhibits FAAH by covalently modifying the enzyme's active site serine nucleophile as expected and is selective for FAAH relative to other mammalian serine hydrolases as demonstrated by activity-based protein profiling (ABPP).<sup>17</sup> In addition, several groups have recently

**Received Date:** August 11, 2010

**Accepted Date:** October 15, 2010

**Published on Web Date:** November 15, 2010

reported apparent noncovalent FAAH inhibitors with no obvious serine-interacting groups (i.e., **8**).<sup>23</sup>



We reasoned that in the case of a target like FAAH, where inhibition leads to elevated levels of endogenous *N*-acyl ethanolamine (NAE) substrates by up to 10–20-fold in central tissues, an irreversible inhibitor may be beneficial because the nonequilibrium binding mechanism limits the competition with high endogenous substrate concentrations leading to increased biochemical efficiency.<sup>24</sup> Furthermore, the pharmacodynamic effect resulting from covalent inhibition often outlasts the pharmacokinetics of the inhibitor, because enzyme activity can be recovered only by synthesis of new enzyme or, in some cases, by slow hydrolysis of the covalent enzyme adduct. To minimize the risk associated with developing a covalent inhibitor, two critical design/screening principles were emphasized—selectivity to avoid off target toxicity and potency to achieve as low a dose as possible.<sup>25</sup>

In this manuscript, we describe the evolution of a series of benzylidene piperidine urea FAAH inhibitors with improved potency and pharmaceutical properties, culminating in the clinical candidate PF-04457845 (**23**). Given the lipophilic nature of the fatty acid amide substrates of FAAH (i.e., *clog P* of anandamide = 6.2), it is not surprising that adding lipophilicity to FAAH inhibitors in the acyl chain binding region improves potency.<sup>26,27</sup> The major challenge is balancing potency with appropriate physicochemical properties to identify FAAH inhibitors with high oral bioavailability that are suitable for clinical development. During the evolution of **23** from **7**, we focused on improving the potency without compromising essential druglike properties.<sup>28</sup> One strategy was to rigidify the conformation of the molecule within the acyl chain binding domain to reduce the entropic penalty of binding by having less rotatable bonds and lowering the conformational energy of the active conformer.<sup>29</sup> Another key area of investigation was focused on finding optimal places in the molecule to incorporate polarity for modulating parameters such as *clog P* and *pK<sub>a</sub>*, while simultaneously optimizing lipophilic interactions within the acyl chain binding pocket.

We initially sought to explore piperidine isosteres with different ring sizes and conformational constraints with the

**Table 1.** Human and Rat FAAH Potency ( $k_{\text{inact}}/K_i$  values) for Piperidine Spacer Analogues<sup>a</sup>

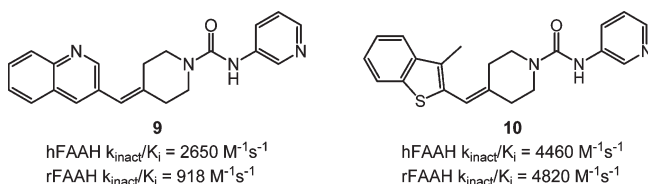
Chemical structure of the general piperidine spacer analogue: A piperidine ring with a benzylidene group at the 2-position and a urea group at the 1-position. The urea group is linked to a biaryl ether moiety (4-(trifluoromethyl)phenoxyphenyl) via an amide bond. The R group is attached to the biaryl ether moiety.

Compd	R	hFAAH $k_{\text{inact}}/K_i$ ( $M^{-1}s^{-1}$ )	rFAAH $k_{\text{inact}}/K_i$ ( $M^{-1}s^{-1}$ )
7		12,600 ± 3000	3900 ± 780
11		21,600 ± 6600	15,100 ± 3400
12		88	NA
13		<16	NA
14		144 ± 47	NA
15		298 ± 110	173 ± 31
16		1150 ± 57	233 ± 17
17		35 ± 6	22 ± 4

<sup>a</sup> Each  $k_{\text{inact}}/K_i$  value corresponds to an average of at least two independent determinations ( $\pm$ SD) and was obtained using the method described in the Supporting Information.

goal of optimally projecting the biaryl ether moiety into the acyl chain binding channel. Because these ureas inhibit FAAH irreversibly, the potency was measured as the second order rate constant  $k_{\text{inact}}/K_i$  using an enzyme-coupled human FAAH (hFAAH) and rat FAAH (rFAAH) assay as described previously.<sup>17,22</sup> Unlike  $IC_{50}$  values,  $k_{\text{inact}}/K_i$  values are independent of preincubation times and substrate concentrations and are considered the best measure of potency for irreversible inhibitors. We found that incorporating a methylenepiperidine into the previous quinoline (i.e., **4**)<sup>16</sup> and benzothiofene (i.e., **5**)<sup>18</sup> urea series to give analogues **9** and **10** resulted in improved FAAH potency, particularly against the rat enzyme. Therefore, we made the corresponding methylenepiperidine analogue in the PF-3845 biaryl ether piperidine series (Table 1). We were gratified to see that methylenepiperidine **11** was approximately 2- and 4-fold more potent than the corresponding methylpiperidine **7** for hFAAH and rFAAH, respectively. Furthermore, **11** was equipotent against the hFAAH and rFAAH enzymes. We also prepared the corresponding pyrrolidine (**12–14**) and azetidine (**15**) analogues, but these were considerably less active. We do not know the precise reason why the activity drops off with smaller ring sizes, but we speculate that the urea is not able to be activated to the same extent upon binding in the FAAH active site.<sup>30</sup> In addition, we prepared the (*E*)- and (*Z*)-3-methylenepiperidine analogues (**16** and **17**). The (*E*)-isomer **16** was approximately 19-fold less potent than **11** for hFAAH, while the activity was almost completely abolished in the case of the

(*Z*)-isomer **17**. On the basis of this data, the 4-methylenepiperidine spacer is optimal in this biarylether urea scaffold.



We next examined the structure–activity relationship (SAR) of the 3-aminopyridyl portion of the molecule, which constitutes the leaving group upon carbamylation of the FAAH active site serine. Our previous work on benzothio-phenone urea FAAH inhibitors indicated that a heteroaryl group was preferred at this position.<sup>18</sup> We were especially interested in introducing substituents next to the pyridyl nitrogen as well as exploring other heterocycle replacements, because of the potential cytochrome P450 metabolic liability associated with unsubstituted pyridines. Indeed, compound **11** exhibited moderate CYP2D6 and CYP3A4 inhibition (Table 2). As observed with previous urea FAAH inhibitors, the 3-aminopyridine analogue (**11**) was superior to the 2-aminopyridine (**18**) and aniline (**19**) analogues. Introduction of a methyl (**20**) or methoxy (**21**) substituent at the 6-position of the 3-aminopyridine provided analogues with slightly reduced potency. The methylpyridine analogue (**20**) had less CYP3A4 inhibition, but the CYP2D6 inhibition was unaffected. We next explored similar heterocycles with reduced basicity while maintaining the position of the nitrogen relative to the 3-aminopyridine. As expected, replacement of the pyridine with the less basic pyrazine (**22**) or pyridazine (**23**) removed any potential CYP liabilities. Unexpectedly, compounds **22** and **23** displayed a 2-fold higher  $k_{\text{inact}}/K_i$  value for hFAAH as compared to **11**. We also assessed several 5-membered and 5,6-fused heterocycles (e.g., **24** and **25**). These compounds generally showed reduced potency for hFAAH but increased potency for rFAAH. For example, the dimethylisoxazole **24** was 5-fold less potent for hFAAH but 2-fold more potent for rFAAH as compared to **23**. This highlights the importance of screening compounds against both the hFAAH and the rFAAH enzymes.<sup>17–18,22</sup> Thus, the benzylidenepiperidine pyridazine urea scaffold appears to be optimal.

We next surveyed the importance of the pyridyl nitrogen as well as the position and nature of the substituent on the left-hand side biaryl ether moiety (Table 3). Removal of the pyridine nitrogen (i.e., compound **26**) resulted in a 2-fold reduction in potency for hFAAH. An additional 10-fold loss in potency resulted from removal of the trifluoromethyl substituent as observed for compound **27**. The trifluoromethyl group at the 5-position of the 2-pyridyl ring makes key van der Waals contacts in the acyl chain-binding pocket that are important for potency in an analogous fashion to that described for PF-3845 (**7**).<sup>17</sup> In contrast, substituents at the 6-position (**34**), 4-position (**32**), or 3-position (**33**) impair potency, demonstrating that steric bulk is not accommodated in that region. The position of the nitrogen in the pyridine ring is also important. Interestingly, the potency of **28** for hFAAH was within 2-fold of

**Table 2.** Human and Rat FAAH Potency ( $k_{\text{inact}}/K_i$  Values) and CYP IC<sub>50</sub> Values for Heteroaryl Urea Analogues<sup>a</sup>

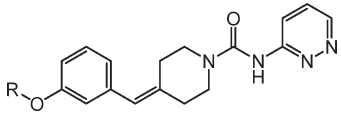
Compd	R	hFAAH $k_{\text{inact}}/K_i$ ( $\text{M}^{-1}\text{s}^{-1}$ )	rFAAH $k_{\text{inact}}/K_i$ ( $\text{M}^{-1}\text{s}^{-1}$ )	CYP inhibition IC <sub>50</sub>	
<b>11</b>		21,600 ± 6600	15,100 ± 3400	2D6	1.4 μM
				3A4 <sup>b</sup>	4.3 μM
				3A4 <sup>c</sup>	0.8 μM
<b>18</b>		6090 ± 3000	563 ± 98		
<b>19</b>	Ph	4800 ± 230	584 ± 34		
<b>20</b>		13,100 ± 5100	5210 ± 1200	2D6	1.6 μM
				3A4 <sup>b</sup>	11.8 μM
				3A4 <sup>c</sup>	3.0 μM
<b>21</b>		16,000 ± 3100	11,400 ± 2900		
<b>22</b>		42,600 ± 16,000	23,700 ± 3800	2D6	25.1 μM
				3A4 <sup>b</sup>	30 μM
				3A4 <sup>c</sup>	23.5 μM
<b>23</b>		40,300 ± 11,000	32,400 ± 8600	2D6	14.5 μM
				3A4 <sup>b</sup>	30 μM
				3A4 <sup>c</sup>	30 μM
<b>24</b>		7990 ± 1600	54,400 ± 14,000		
<b>25</b>		3930 ± 380	30,200 ± 7200		

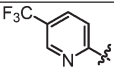
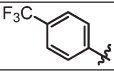
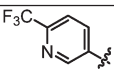
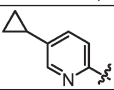
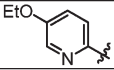
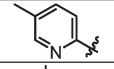
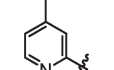
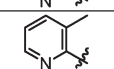
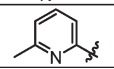
<sup>a</sup> Each  $k_{\text{inact}}/K_i$  value corresponds to an average of at least two independent determinations ( $\pm$ SD) and was obtained using the method described in the Supporting Information. <sup>b</sup> Midazolam was used as the CYP3A4 substrate. <sup>c</sup> Testosterone was used as the CYP3A4 substrate.

**23**, but the potency for rFAAH was dramatically reduced. Finally, several other substituents were shown to be tolerated at the 5-position (i.e., **29–31**), and the trifluoromethyl group proved to be optimal.

These medicinal chemistry efforts culminated in the discovery of PF-04457845 (compound **23**, Table 2), a benzylidenepiperidine pyridazine urea that displayed a 3- and 8-fold higher  $k_{\text{inact}}/K_i$  value for hFAAH and rFAAH, respectively, as compared to PF-3845 (**7**). We also measured FAAH potency for **23** by determining IC<sub>50</sub> values with a 60 min preincubation time, and the IC<sub>50</sub> was  $7.2 \pm 0.63 \text{ nM}$  for hFAAH and  $7.4 \pm 0.62 \text{ nM}$  for rFAAH (see the Supporting Information). Key features of **23** that contribute to its potency include the *p*-trifluoromethyl substituent and the pyridyl nitrogen on the biaryl ether moiety, the benzylidenepiperidine urea, and the 3-aminopyridazine leaving group. It is worthwhile to note that not only did the pyridine and pyridazine heterocycles contribute to the improved potency, but they also served to lower the lipophilicity and improve the physicochemical properties (i.e.,  $\text{clog } P = 3.9$ ,  $\text{PSA} = 80$ ) and ADME parameters (vide supra) for **23**.

PF-04457845 (**23**) was synthesized in six linear steps with a 40% overall yield from commercially available starting

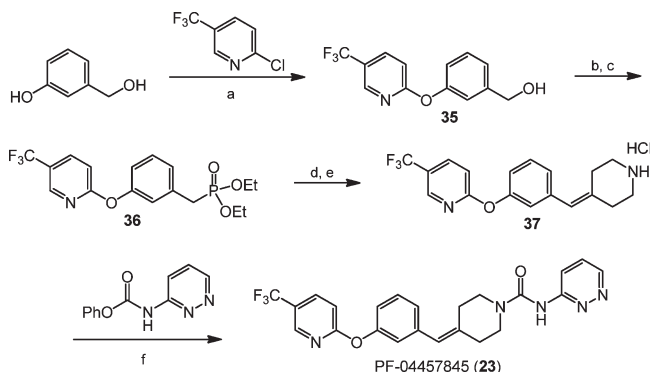
**Table 3.** Human and Rat FAAH Potency ( $k_{\text{inact}}/K_i$  Values) of Biaryl Ether Analogues<sup>a</sup>

Compd	R	hFAAH $k_{\text{inact}}/K_i$ ( $\text{M}^{-1}\text{s}^{-1}$ )	rFAAH $k_{\text{inact}}/K_i$ ( $\text{M}^{-1}\text{s}^{-1}$ )
<b>23</b>		40,300 ± 11,000	32,400 ± 8600
<b>26</b>		18,900 ± 3500	22,900 ± 7600
<b>27</b>	Ph	1530 ± 300	1900 ± 220
<b>28</b>		26,600 ± 5100	2020 ± 450
<b>29</b>		28,800 ± 5400	46,300 ± 19,000
<b>30</b>		9230 ± 2200	11,700
<b>31</b>		21,500 ± 9200	5530 ± 1800
<b>32</b>		1580 ± 590	-
<b>33</b>		2200 ± 240	256 ± 75
<b>34</b>		1090 ± 260	586 ± 100

<sup>a</sup> Each  $k_{\text{inact}}/K_i$  value corresponds to an average of at least two independent determinations ( $\pm$ SD) and was obtained using the method described in the Supporting Information.

materials (Scheme 1). The synthesis began with a nucleophilic aromatic substitution of 3-(hydroxymethyl)phenol with 2-chloro-5-(trifluoromethyl)pyridine in the presence of  $\text{K}_2\text{CO}_3$  to form biaryl ether **35**. Treatment of benzyl alcohol **35** with thionyl chloride provided the corresponding benzyl chloride, which was reacted with triethyl phosphite to give the benzylphosphonate **36**. Horner–Wadsworth–Emmons olefination of 1-Boc-4-piperidone with **36** in the presence of potassium *tert*-butoxide followed by removal of the Boc protecting group using HCl in dioxane afforded the benzylidene-piperidine **37** as the hydrochloride salt. Finally, reaction of **37** with phenyl pyridazin-3-ylcarbamate in the presence of diisopropylethyl amine provided the urea **23**.

We next assessed the selectivity of PF-04457845 (**23**) against the serine hydrolase superfamily of enzymes (> 200 members in humans) of which FAAH is a member.<sup>16–18</sup> Compound **23** was profiled at 10 and 100  $\mu\text{M}$  utilizing a functional proteomic screen based on competitive activity-based protein profiling (ABPP)<sup>31</sup> in brain membrane and soluble liver proteomes derived from both human and mouse. We used a rhodamine-tagged fluorophosphonate (FP) ABPP probe, which serves as a general activity-based profiling tool for the serine hydrolase superfamily.<sup>32</sup> Serine hydrolases that show significant reductions in FP probe

**Scheme 1.** Synthesis of PF-04457845 (**23**)<sup>a</sup>

<sup>a</sup> Reagents and conditions: (a)  $\text{K}_2\text{CO}_3$ , DMF, 90–95 °C, 16 h, quant. (b)  $\text{SOCl}_2$ ,  $\text{CH}_2\text{Cl}_2$ , room temperature, 2 h, quant. (c)  $\text{P}(\text{OEt})_3$ , 130 °C, 16 h, 80%. (d) *N*-Boc-piperidin-4-one, *t*-BuOK, THF, 69%. (e) HCl, dioxane, 84%. (f) *i*-Pr<sub>2</sub>NEt,  $\text{CH}_3\text{CN}$ , RT, 16 h, 86%.

labeling intensity in the presence of inhibitor are scored as targets of the compound. The selectivity of **23** was compared to that of the carbamate FAAH inhibitor URB597 (**2**) (Figure 1). Both **23** and **2** completely inhibited FAAH in human and mouse membrane proteomes at both 10 and 100  $\mu\text{M}$  with no off targets. However, in soluble proteomes of liver, the profile of **23** was drastically different than that of **2**. Compound **23** was completely selective as none of the other FP-reactive serine hydrolases were inhibited even at 100  $\mu\text{M}$ . In contrast, **2** displayed multiple off targets as it blocked FP labeling of several additional serine hydrolases, particularly among FP-labeled proteins migrating between 55 and 65 kDa. Several off targets were completely inhibited even at 10  $\mu\text{M}$  **2**. Thus, **23** is exquisitely selective for FAAH relative to other mammalian serine hydrolases. In addition, **23** exhibited a favorable selectivity profile when screened against a 68 target CEREP panel (Table S1 in the Supporting Information).

PF-04457845 (**23**) has an excellent pharmacokinetic profile in rats and dogs as well as in human *in vitro* assays. The permeability of **23** (A-B,  $15.2 \times 10^{-6}$  cm/s; and B-A,  $20.2 \times 10^{-6}$  cm/s) across MDCK cells was moderate, with no apparent efflux due to Pgp (B/A ratio is 1.33). Compound **23** has low clearance and moderate volume of distribution in rats and dogs (Table 4). Compound **23** was rapidly absorbed following oral administration of a methylcellulose suspension of the crystalline material with a bioavailability of 88% in rats and 58% in dogs. Low risk for drug–drug interactions is anticipated based on *in vitro* CYP inhibition studies in human liver microsomes using relevant substrates (Table S2 in the Supporting Information). The potential of **23** to form reactive metabolites was investigated, and no glutathione conjugate of **23** was observed from *in vitro* rat or human hepatocyte incubations. The half-life of **23** in human liver microsomal experiments was determined to be 105 min tested at 0.8 mg/mL protein concentration. The microsomal protein binding of **23** was 90%. Human blood clearance based on these *in vitro* experiments was predicted to be 0.6 mL/min/kg. On the basis of this data, **23** is predicted to be suitable for once a day oral administration in humans.

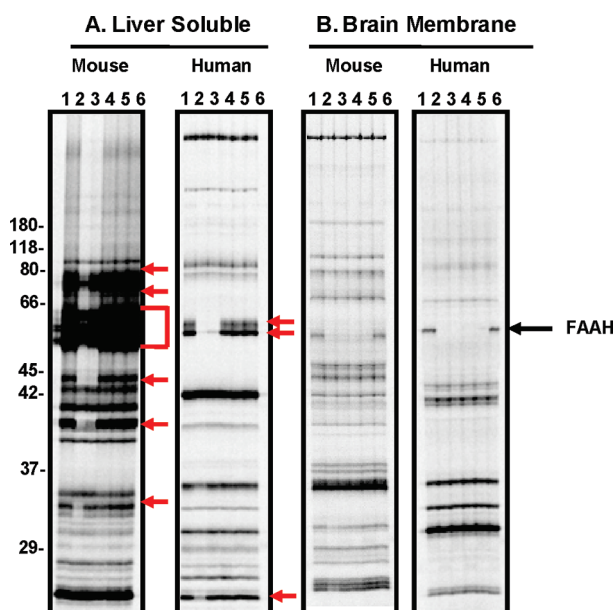


**Figure 1.** Selectivity profiling of PF-04457845 (**23**) and URB597 (**2**) by competitive ABPP. Gel images of proteomes labeled with FP-rhodamine in the presence or absence of FAAH inhibitors (lane 1, DMSO; lane 2, **2** at 100  $\mu$ M; lane 3, **2** at 10  $\mu$ M; lane 4, **23** at 100  $\mu$ M; lane 5, **23** at 10  $\mu$ M; and lane 6, DMSO). Gel profiles of FP-rhodamine-labeled mouse and human (A) liver soluble serine hydrolases and (B) brain membrane serine hydrolases in the presence or absence of **23** and **2**. The band on the gel corresponding to the FAAH enzyme is highlighted by the black arrow. Note that **2**, but not **23**, blocks FP-rhodamine labeling of several liver serine hydrolases (red arrows and bracket). For both A and B, fluorescent gel images are shown in grayscale.

We next assessed *in vivo* efficacy of PF-04457845 (**23**) in a rat model of inflammatory pain. Subcutaneous injection of complete Freund's adjuvant (CFA) into the plantar surface of the hind paw produced a significant decrease in mechanical paw withdrawal threshold (PWT) after 5 days postinjection as previously described (Figure 2).<sup>17</sup> Oral administration of **23** caused a significant inhibition of mechanical allodynia measured after 4 h with a minimum effective dose (MED) of 0.1 mg/kg, which is  $\sim$ 30-fold lower than PF-3845 (**7**) (MED of 3 mg/kg). Furthermore, at 0.1 mg/kg (p.o.), **23** inhibited the pain response to a comparable degree as the nonsteroidal anti-inflammatory drug naproxen at 10 mg/kg (Figure 2). It has been reported that a near-complete blockade of FAAH activity is required to maintain elevated anandamide levels *in vivo*.<sup>14,17</sup> In full agreement with this observation, the robust *in vivo* efficacy by **23** was accompanied by near complete inhibition of FAAH activity with concomitant elevations in anandamide and other fatty acid amides in brain and plasma (details will be described elsewhere). The degree of inhibition in pain response by **23** was similar at all efficacious doses likely because near complete FAAH inhibition is necessary to obtain *in vivo* efficacy, which was achieved at all doses starting at 0.1 mg/kg.

In conclusion, PF-04457845 (**23**) is a potent FAAH inhibitor that covalently modifies the active-site serine nucleophile of FAAH with exquisite selectivity relative to other members of the serine hydrolase superfamily. The compound

**Table 4.** Plasma Pharmacokinetic Data Following Administration of PF-04457845 (**23**) (iv<sup>a</sup> and po<sup>b</sup> Dose of 1 mg/kg in Rat and 0.5 mg/kg in Dog)

species	oral $C_{max}$ (ng/mL)	$t_{max}$ (h)	CL (mL/min/kg)	$Vd_{ss}$ (L/kg)	iv $t_{1/2}$ (h)	% F
rat	256	4.0	3.0	3.2	14.3	88
dog	240	1.0	1.3	2.9	35.2	58

<sup>a</sup> Intravenous doses were formulated in 5% dimethylacetamide and 95% (40% SBE-cyclodextrin in water). <sup>b</sup> Oral doses were formulated in 5% (0.1% Tween 80) and 95% (0.5% methylcellulose).

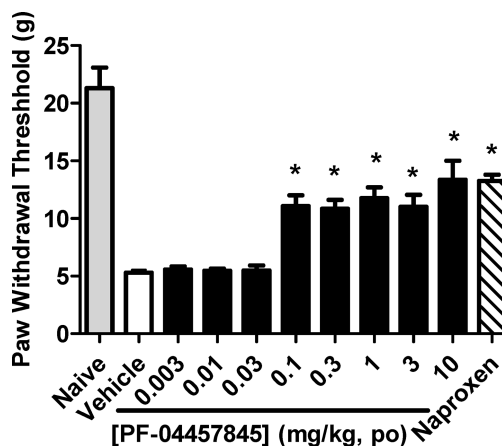


**Figure 2.** Antihyperalgesic effects of PF-04457845 (**23**) in the CFA model of inflammatory pain in rats. Compound **23**, at 0.1 to 10 mg/kg (po), produced a reduction of mechanical allodynia (hyperalgesia) in rats (black bars). The effect of the nonsteroidal anti-inflammatory drug naproxen (10 mg/kg, po, hatched bar) is shown for comparison. The antihyperalgesic responses were determined at 4 h following drug treatment and were significantly different for **23** (0.1–10 mg/kg, po) and naproxen (10 mg/kg, po) as compared to vehicle-treated groups ( $p < 0.05$ ),  $n = 8$  rats per group.

has excellent pharmacokinetic properties and is suitable for once a day oral administration. It is efficacious in the CFA model of inflammatory pain in rats. Compound **23** is currently being evaluated in human clinical trials with the potential to treat chronic pain and other nervous system disorders.

**SUPPORTING INFORMATION AVAILABLE** Experimental procedures for the synthesis of **11–34**, assay protocols, and two supplementary tables. This material is available free of charge via the Internet at <http://pubs.acs.org>.

#### AUTHOR INFORMATION

**Corresponding Author:** \*E-mail: doug.johnson@pfizer.com.

#### REFERENCES

- Cravatt, B. F.; Giang, D. K.; Mayfield, S. P.; Boger, D. L.; Lerner, R. A.; Gilula, N. B. Molecular characterization of an enzyme that degrades neuromodulatory fatty-acid amides. *Nature* **1996**, *384*, 83–87.
- McKinney, M. K.; Cravatt, B. F. Structure and function of fatty acid amide hydrolase. *Annu. Rev. Biochem.* **2005**, *74*, 411–432.
- Ahn, K.; McKinney, M. K.; Cravatt, B. F. Enzymatic pathways that regulate endocannabinoid signaling in the nervous system. *Chem. Rev.* **2008**, *108*, 1687–1707.
- Patricelli, M. P.; Cravatt, B. F. Fatty acid amide hydrolase competitively degrades bioactive amides and esters through

- a nonconventional catalytic mechanism. *Biochemistry* **1999**, *38*, 14125–14130.
- (5) Ezzili, C.; Otrubova, K.; Boger, D. L. Fatty acid amide signaling molecules. *Bioorg. Med. Chem. Lett.* **2010**, *20*, 5959–5968.
- (6) Cravatt, B. F.; Demarest, K.; Patricelli, M. P.; Bracey, M. H.; Giang, D. K.; Martin, B. R.; Lichtman, A. H. Supersensitivity to anandamide and enhanced endogenous cannabinoid signaling in mice lacking fatty acid amide hydrolase. *Proc. Natl. Acad. Sci. U.S.A.* **2001**, *98*, 9371–9376.
- (7) Cravatt, B. F.; Saghatelian, A.; Hawkins, E. G.; Clement, A. B.; Bracey, M. H.; Lichtman, A. H. Functional disassociation of the central and peripheral fatty acid amide signaling systems. *Proc. Natl. Acad. Sci. U.S.A.* **2004**, *101*, 10821–10826.
- (8) Ahn, K.; Johnson, D. S.; Cravatt, B. F. Fatty acid amide hydrolase as a potential therapeutic target for the treatment of pain and CNS disorders. *Expert Opin. Drug Discovery* **2009**, *4*, 763–784.
- (9) Petrosino, S.; Di Marzo, V. FAAH and MAGL inhibitors: Therapeutic opportunities from regulating endocannabinoid levels. *Curr. Opin. Invest. Drugs* **2010**, *11*, 51–62.
- (10) Seierstad, M.; Breitenbucher, J. G. Discovery and Development of Fatty Acid Amide Hydrolase (FAAH) Inhibitors. *J. Med. Chem.* **2008**, *51*, 7327–7343.
- (11) Boger, D. L.; Miyauchi, H.; Du, W.; Hardouin, C.; Fecik, R. A.; Cheng, H.; Hwang, I.; Hedrick, M. P.; Leung, D.; Acevedo, O.; Guimaraes, C. R.; Jorgensen, W. L.; Cravatt, B. F. Discovery of a potent, selective, and efficacious class of reversible alpha-ketoheterocycle inhibitors of fatty acid amide hydrolase effective as analgesics. *J. Med. Chem.* **2005**, *48*, 1849–1856.
- (12) Mileni, M.; Garfunkle, J.; DeMartino, J. K.; Cravatt, B. F.; Boger, D. L.; Stevens, R. C. Binding and inactivation mechanism of a humanized fatty acid amide hydrolase by alpha-ketoheterocycle inhibitors revealed from cocrystal structures. *J. Am. Chem. Soc.* **2009**, *131*, 10497–10506.
- (13) Mor, M.; Rivara, S.; Lodola, A.; Plazzi, P. V.; Tarzia, G.; Duranti, A.; Tontini, A.; Piersanti, G.; Kathuria, S.; Piomelli, D. Cyclohexylcarbamic acid 3'- or 4'-substituted biphenyl-3-yl esters as fatty acid amide hydrolase inhibitors: Synthesis, quantitative structure-activity relationships, and molecular modeling studies. *J. Med. Chem.* **2004**, *47*, 4998–5008.
- (14) Fegley, D.; Gaetani, S.; Duranti, A.; Tontini, A.; Mor, M.; Tarzia, G.; Piomelli, D. Characterization of the fatty acid amide hydrolase inhibitor cyclohexyl carbamic acid 3'-carbamoyl-biphenyl-3-yl ester (URB597): Effects on anandamide and oleylethanolamide deactivation. *J. Pharmacol. Exp. Ther.* **2005**, *313*, 352–358.
- (15) Mileni, M.; Kamtekar, S.; Wood, D. C.; Benson, T. E.; Cravatt, B. F.; Stevens, R. C. Crystal Structures of Fatty Acid Amide Hydrolase Bound to the Carbamate Inhibitor URB597: Discovery of a Deacylating Water Molecule and Insight into Enzyme Inactivation. *J. Mol. Biol.* **2010**, *400*, 743–754.
- (16) Ahn, K.; Johnson, D. S.; Fitzgerald, L. R.; Liimatta, M.; Arendse, A.; Stevenson, T.; Lund, E. T.; Nugent, R. A.; Nomanbhoy, T. K.; Alexander, J. P.; Cravatt, B. F. Novel mechanistic class of fatty acid amide hydrolase inhibitors with remarkable selectivity. *Biochemistry* **2007**, *46*, 13019–13030.
- (17) Ahn, K.; Johnson, D. S.; Mileni, M.; Beidler, D.; Long, J. Z.; McKinney, M. K.; Weerapana, E.; Sadagopan, N.; Liimatta, M.; Smith, S. E.; Lazerwith, S.; Stiff, C.; Kamtekar, S.; Bhattacharya, K.; Zhang, Y.; Swaney, S.; Van Becelaere, K.; Stevens, R. C.; Cravatt, B. F. Discovery and characterization of a highly selective FAAH inhibitor that reduces inflammatory pain. *Chem. Biol.* **2009**, *16*, 411–420.
- (18) Johnson, D. S.; Ahn, K.; Kesten, S.; Lazerwith, S. E.; Song, Y.; Morris, M.; Fay, L.; Gregory, T.; Stiff, C.; Dunbar, J. B., Jr.; Liimatta, M.; Beidler, D.; Smith, S.; Nomanbhoy, T. K.; Cravatt, B. F. Benzothioephene piperazine and piperidine urea inhibitors of fatty acid amide hydrolase (FAAH). *Bioorg. Med. Chem. Lett.* **2009**, *19*, 2865–2869.
- (19) Keith, J. M.; Apodaca, R.; Xiao, W.; Seierstad, M.; Pattabiraman, K.; Wu, J.; Webb, M.; Karbarz, M. J.; Brown, S.; Wilson, S.; Scott, B.; Tham, C. S.; Luo, L.; Palmer, J.; Wennerholm, M.; Chaplan, S.; Breitenbucher, J. G. Thiadiazolopiperazinyl ureas as inhibitors of fatty acid amide hydrolase. *Bioorg. Med. Chem. Lett.* **2008**, *18*, 4838–4843.
- (20) Matsumoto, T.; Kori, M.; Miyazaki, J.; Kiyota, Y. Preparation of piperidinecarboxamides and piperazinecarboxamides as fatty acid amide hydrolase (FAAH) inhibitors. WO 2006/054652, 2006.
- (21) Apodaca, R.; Breitenbucher, J. G.; Pattabiraman, K.; Seierstad, M.; Xiao, W. Piperazinyl and piperidinyl ureas as modulators of fatty acid amide hydrolase. WO 2006/074025, 2006.
- (22) Mileni, M.; Johnson, D. S.; Wang, Z.; Everdeen, D. S.; Liimatta, M.; Pabst, B.; Bhattacharya, K.; Nugent, R. A.; Kamtekar, S.; Cravatt, B. F.; Ahn, K.; Stevens, R. C. Structure-guided inhibitor design for human FAAH by interspecies active site conversion. *Proc. Natl. Acad. Sci. U.S.A.* **2008**, *105*, 12820–12824.
- (23) Wang, X.; Sarris, K.; Kage, K.; Zhang, D.; Brown, S. P.; Kolasa, T.; Surowy, C.; El Kouhen, O. F.; Muchmore, S. W.; Brioni, J. D.; Stewart, A. O. Synthesis and evaluation of benzothiazole-based analogues as novel, potent, and selective fatty acid amide hydrolase inhibitors. *J. Med. Chem.* **2009**, *52*, 170–180.
- (24) Swinney, D. C. Biochemical mechanisms of drug action: what does it take for success? *Nat. Rev. Drug Discovery* **2004**, *3*, 801–808.
- (25) Johnson, D. S.; Weerapana, E.; Cravatt, B. F. Strategies for discovering and derisking covalent, irreversible enzyme inhibitors. *Future Med. Chem.* **2010**, *2*, 949–964.
- (26) Sit, S. Y.; Conway, C. M.; Xie, K.; Bertekap, R.; Bourin, C.; Burris, K. D. Oxime Carbamate-Discovery of a series of novel FAAH inhibitors. *Bioorg. Med. Chem. Lett.* **2010**, *20*, 1272–1277.
- (27) Morphy, R. The influence of target family and functional activity on the physicochemical properties of pre-clinical compounds. *J. Med. Chem.* **2006**, *49*, 2969–2978.
- (28) Leeson, P. D.; Springthorpe, B. The influence of drug-like concepts on decision-making in medicinal chemistry. *Nat. Rev. Drug Discovery* **2007**, *6*, 881–890.
- (29) Andrews, P. R.; Craik, D. J.; Martin, J. L. Functional group contributions to drug-receptor interactions. *J. Med. Chem.* **1984**, *27*, 1648–1657.
- (30) We have proposed that the urea may be activated upon binding in the active site of FAAH by undergoing a conformational change that diminishes conjugation of the nitrogen lone pair with the carbonyl, which would activate the urea for attack by the serine nucleophile (see refs 16 and 18).
- (31) Cravatt, B. F.; Wright, A. T.; Kozarich, J. W. Activity-based protein profiling: from enzyme chemistry to proteomic chemistry. *Annu. Rev. Biochem.* **2008**, *77*, 383–414.
- (32) Liu, Y.; Patricelli, M. P.; Cravatt, B. F. Activity-based protein profiling: the serine hydrolases. *Proc. Natl. Acad. Sci. U.S.A.* **1999**, *96*, 14694–14699.

**NOTE ADDED AFTER ASAP PUBLICATION** This paper was published on the Web on November 15, 2010 with an error in structure PF-750 (4). The corrected version was reposted on January 19, 2011.